⌘ *Author's Choice*

THE JOURNAL OF BIOLOGICAL CHEMISTRY VOL. 286, NO. 49, pp. 42514–42523, December 9, 2011

γ-Secretase and Presenilin Mediate Cleavage and Phosphorylation of Vascular Endothelial Growth Factor Receptor-1*

Received for publication, August 22, 2011, and in revised form, October 14, 2011 Published, JBC Papers in Press, October 20, 2011, DOI 10.1074/jbc.M111.296590

Jun Cai[‡], Zhijuan Chen[‡], Qing Ruan[‡], Song Han[§], Li Liu[¶], Xiaoping Qi[‡], Sanford L. Boye[‖], William W. Hauswirth[‖1], Maria B. Grant[¶], and Michael E. Boulton[‡2]

From the Departments of [‡]Anatomy and Cell Biology, [§]Surgery, [¶]Pharmacology and Therapeutics, and [‖]Ophthalmology, University of Florida, Gainesville, Florida 32610-0235

Background: γ-Secretase regulates VEGFR1 signaling.
Results: Transmembrane cleavage of VEGFR1 occurs at valine 767, and VE-PTP dephosphorylation of activated VEGFR1 requires full-length presenilin 1.
Conclusion: γ-Secretase cleaves VEGFR1, and full-length presenilin is a critical adaptor molecule in the dephosphorylation of VEGFR1.
Significance: A greater understanding of PEDF-mediated VEGFR1 signaling and the role of γ-secretase/presenilin in the regulation of angiogenesis is important for cell biology.

We have reported previously that pigment epithelium-derived factor (PEDF) can, via γ-secretase-mediated events, inhibit VEGF-induced angiogenesis in microvascular endothelial cells by both (*a*) cleavage and intracellular translocation of a C-terminal fragment of VEGF receptor-1 (VEGFR1) and (*b*) inhibition of VEGF-induced phosphorylation of VEGFR1. Using site-direct mutagenesis and transfection of wild type and mutated receptors into endothelial cells, we showed that transmembrane cleavage of VEGFR1 occurs at valine 767 and that a switch from valine to alanine at this position prevented cleavage and formation of a VEGFR1 intracellular fragment. Using siRNA to selectively knock down protein-tyrosine phosphatases (PTPs) in endothelial cells, we demonstrated that vascular endothelial PTP is responsible for dephosphorylation of activated VEGFR1. PEDF up-regulation of full-length presenilin 1 (Fl.PS1) facilitated the association of vascular endothelial PTP and VEGFR1. Knockdown of Fl.PS1 prevented dephosphorylation of VEGFR1, whereas up-regulation of Fl.PS1 stimulated VEGFR1 dephosphorylation. Fl.PS1 associated with VEGFR1 within 15 min after PEDF treatment. In conclusion, we determined the PEDF-mediated events responsible for VEGFR1 signaling and identified full-length presenilin as a critical adaptor molecule in the dephosphorylation of VEGFR1. This greater understanding of the regulation of VEGFR1 signaling will help identify novel anti-VEGF therapeutic strategies.

Vascular endothelial growth factor-A (VEGF-A) is a key regulator of both physiological angiogenesis and pathological neovascularization associated with diseases including diabetic complications, cancer, and macular degeneration (1, 2). VEGF-A binds to two different receptor tyrosine kinases, namely VEGFR1[3] (flt-1) and VEGFR2 (flk-1/kinase insert domain receptor), which are both expressed on vascular endothelial cells (3). VEGFR1 and VEGFR2 are structurally similar, consisting of an extracellular ligand-binding domain with seven immunoglobulin (Ig)-like motifs, a transmembrane domain (TMD), a kinase domain split by a kinase insert, and a C terminus. Overall, there is 43.2% amino acid sequence homology between VEGFR1 and VEGFR2, and VEGF-A binds to VEGFR1 with higher affinity than to VEGFR2 (4). The classic view is that VEGFR2 regulates endothelial function and survival via a number of different canonical signaling pathways including Ras/mitogen-activated protein kinase (MAPK), Src, PI3K, and NOS (3), although this can be further modified through receptor heterodimerization and association with co-receptors neuropilin-1 and -2. However, VEGFR1 signaling is more complex because it (*a*) has only very weak kinase activity when compared with VEGFR2 (4), (*b*) is both a positive and negative regulator of angiogenesis depending on the particular ligand binding (pla-

* This work was supported, in whole or in part, by National Institutes of Health Grants R01EY018358 and R01EY018358-04S1 (to M. B.), EY012601 and DK090730 (to M. B. G.), and R01EY11123 and P30EY021721 (to W. W. H.). W. W. H. and the University of Florida have a financial interest in the use of AAV therapies and own equity in a company (AGTC Inc.) that might, in the future, commercialize some aspects of this work.

⌘ *Author's Choice*—Final version full access.

[1] Supported by grants from the Macular Vision Research Foundation, Foundation Fighting Blindness, Eldon Family Foundation, Vision for Children, and Research to Prevent Blindness, Inc.

[2] To whom correspondence should be addressed: Dept. of Anatomy and Cell Biology, University of Florida, 1600 S. W. Archer Rd., P. O. Box 100235, Gainesville, FL 32610-0235. Tel.: 352-273-8546; Fax: 352-846-1248; E-mail: meboulton@ufl.edu.

[3] The abbreviations used are: VEGFR, vascular endothelial growth factor receptor; AAV, adeno-associated virus; BRMECs, bovine retinal microvascular endothelial cells; CTF, C-terminal fragment; Fl.PS, full-length presenilin; ICD, intracellular domain; NCT, nicastrin; PAEC, porcine aortic endothelial cell; PEDF, pigment epithelium-derived factor; PS, presenilin; PTP, protein-tyrosine phosphatase; RIP, regulated intramembrane proteolysis; TMD, transmembrane domain; VEcad, vascular endothelial cadherin; VE-PTP, vascular endothelial protein-tyrosine phosphatase; DAPT, *N*-[*N*-(3,5-difluorophenacetyl)-L-alanyl]-*S*-phenylglycine *t*-butyl ester; TRITC, tetramethylrhodamine isothiocyanate; SHP, Src homology 2 domain-containing PTP.

centa growth factor-1 inhibits angiogenesis, whereas VEGF and placenta growth factor-2 are proangiogenic) (5), (*c*) can heterodimerize with VEGFR2 (4), and (d) participates in the antiangiogenic activity of pigment epithelium-derived factor (PEDF) (6, 7).

PEDF is a potent endogenous antiangiogenic factor that can inhibit VEGF-induced permeability and angiogenesis (6, 8). Previously, we have shown that this effect is in part due to γ-secretase-dependent regulation of the cleavage and translocation of VEGFR1 because PEDF action is blocked by either pharmacological inhibition of γ-secretase or by siRNA inhibition of γ-secretase (7, 8). Furthermore, Rahimi *et al.* (9) have reported that γ-secretase can cleave VEGFR1 in cancer cells. γ-Secretase is a complex composed of four different integral proteins (presenilin, nicastrin, APH-1, and PEN-2) (6). The most studied components of the γ-secretase complex are presenilin (PS), an integral enzyme in the transmembrane cleavage of substrates, and nicastrin (NCT), which is essential for substrate recognition (6). Activation of PS is dependent on its endoproteolysis into an N-terminal fragment and C-terminal fragment (CTF) (6). Recently, it has been proposed that components of γ-secretase, in particular PS, can operate independently of the γ-secretase complex and act as adaptor proteins to facilitate protein-protein interactions (6, 10, 11). We have shown previously that PEDF can inhibit VEGF-induced angiogenesis in microvascular endothelial cells by both (*a*) cleavage and intracellular translocation of a C-terminal fragment of VEGFR1 and (*b*) inhibition of VEGF-induced phosphorylation of VEGFR1 (7).

Regulated intramembrane proteolysis (RIP) has emerged as an important mechanism in signal transduction and degradation of transmembrane proteins (12). RIP has been described for a number of transmembrane proteins including Notch, amyloid precursor protein, and a number of receptor tyrosine kinases (6, 13–15). In general, RIP processing involves an initial ectodomain shedding followed by secondary cleavage in the TMD by γ-secretase to release an intracellular domain.

Protein-tyrosine phosphatases (PTPs) are potent enzyme regulators of receptor tyrosine kinases that catalyze the dephosphorylation of tyrosine phosphorylated proteins (16, 17). The specificity of the PTPs relies on the recognition of certain phosphopeptides for their action and on the selective expression of individual PTPs. Our previous study showed that Src homology 2 domain-containing PTPs SHP1 (PTP1C) and SHP2 (PTP1D) are important for the dephosphorylation of VEGFR2 (18), and more recently, a vascular endothelial protein-tyrosine phosphatase (VE-PTP/PTPRB) has been identified (19). However, although much is known about dephosphorylation of VEGFR2, little is known regarding dephosphorylation of VEGFR1. In this study, we identified the VEGFR1 transmembrane cleavage site for γ-secretase and determined the mechanism by which PEDF induces dephosphorylation of VEGFR1.

EXPERIMENTAL PROCEDURES

Cell Culture—Bovine retinal microvascular endothelial cells (BRMECs) were isolated and cultured as described previously (7). Briefly, freshly isolated bovine retinas were homogenized, and after trapping on an 83-μm nylon mesh,

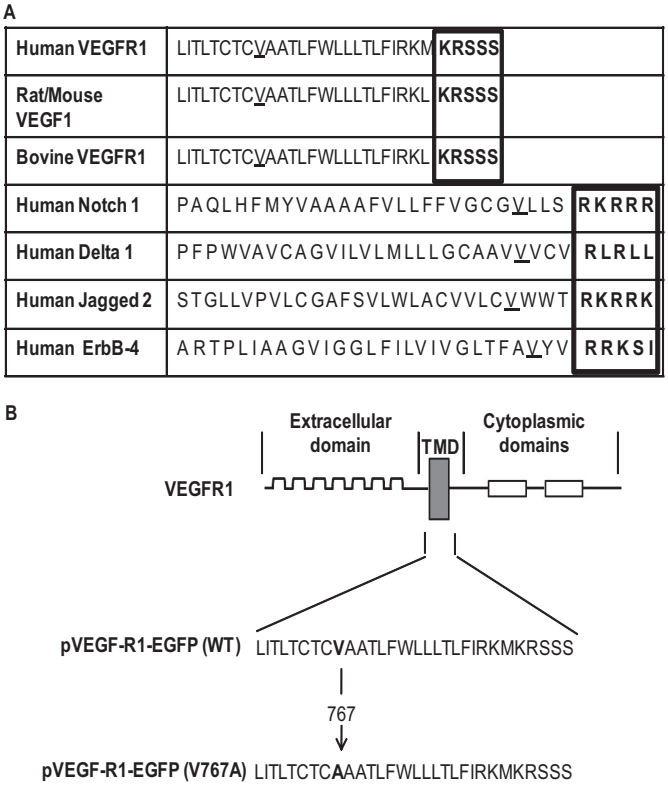

FIGURE 1. **Schematic presentation of TMD of VEGFR1 and proposed γ-secretase cleavage site.** *A*, TMD sequences of VEGFR1 compared with known γ-secretase transmembrane cleavage sites for Notch, Delta, Jagged, and ErbB4. Note the conserved valine (*underlined*) and charged residues immediately downstream (*boxed*). *B*, human VEGFR1 transmembrane sequence showing the generation of mutant pVEGF-R1-EGFP by exchanging the valine 767 residue of the TMD for alanine.

they were transferred into an enzyme mixture (500 μg/ml collagenase, 200 μg/ml Pronase, and 200 μg/ml DNase) at 37 °C for 20 min. The resultant vessel fragments were trapped on a 53-μm mesh, washed, and pelleted, and cells were plated in endothelial cell basal medium with growth supplement (Invitrogen) at 37 °C in 5% CO_2 for 3 days. The cells were used within three passages.

γ-Secretase Activity—The γ-secretase activity was assessed in total cell lysates using the γ-Secretase Activity kit (R&D Systems, Minneapolis, MN) as described previously (7).

Plasmid Constructs—cDNA encoding full-length *VEGFR1* was obtained by polymerase chain reaction (PCR) from human umbilical vein endothelial cells. To generate vectors for stable expression of VEGFR1, the PCR product was ligated into TOPO cloning vector (Invitrogen) according to the manufacturer's instructions and was subcloned into the pEGFP-N1 vector; the C terminus of VEGFR1 was tagged with a sequence corresponding to the N terminus of green fluorescent protein (GFP). pEGFP-N1, containing the CMV promoter, kanamycin resistance gene, and GFP gene, was purchased from Clontech. The construct encoding GFP fused to VEGFR1 was obtained by inserting the complete human VEGFR1 sequence between HindIII (1.3 kbp) and HindIII (2.9 kbp) sites of pEGFP-N1. The resulting vector was named pVEGF-R1-EGFP wild type (WT). Correct insertion was verified by DNA sequencing. Mutagenesis was performed with sets of primers. The valine 767 residue

of the TMD of human VEGFR1 was mutated to an alanine residue (Fig. 1, *A* and *B*) using the oligonucleotides 5′-TCACTCTAACATGCACCTGTCCTGCTGCGACTCT-3′ and 5′-ACAGGTGCATGTTAGAGTGATCAGCTCCAGATTA-3′ with a XL site-directed mutagenesis kit (Stratagene, La Jolla, CA). The mutations were confirmed by DNA sequencing, and mutant VEGFR1 was cloned into the plasmid pEGFP-N1. The resultant vector was referred to as pVEGF-R1-EGFP mutant (V767A).

Generation of Endothelial Cell Lines Stably Expressing VEGFR1—Porcine aortic endothelial cells (PAECs) lacking expression of both VEGFR1 and VEGFR2 were purchased from Cell Application (San Diego, CA) and cultured in endothelial basal medium with growth supplement (Invitrogen) in 6-well plates precoated with endothelial attachment factor (Invitrogen). Transfection of pVEGF-R1-EGFP was performed with Lipofectamine™ LTX and Plus™ reagents (Invitrogen). After transfection, the cells were cultured in antibiotic-free endothelial basal medium with growth supplement for 24 h before the Lipofectamine-containing medium was replaced with fresh endothelial basal medium with growth supplement containing kanamycin sulfate (50 mg/ml) for selection of stable cell lines expressing VEGR1.

Growth Factor and γ-Secretase Inhibitor Treatments—Endothelial cell cultures were rendered quiescent for 45 min in serum-free basal medium. VEGF and PEDF (alone or in combination) were added at 100 ng/ml based on our previous studies (7, 8). Experiments were undertaken in the presence or absence of 1 nM γ-secretase inhibitor DAPT (Sigma). Cells were analyzed after varying time periods as described below. In some of the cleavage studies, the proteasomal inhibitor lactacystin (Sigma) was used (5 and 10 μM) to prevent degradation of VEGFR1 fragments.

Subcellular Protein Extraction—Membrane and cytosolic proteins were purified from endothelial cells using the ProteoExtract™ subcellular proteome extraction kit (EMD Chemicals, Gibbstown, NJ). This kit preserves the integrity of the subcellular structures before and during extraction to prevent any mixing of the different subcellular compartments.

Immunoprecipitation and Western Blotting—Immunoprecipitation and Western blotting were performed as described previously (5, 7, 8). In brief, cells were lysed in radioimmunoprecipitation assay buffer containing protease and phosphatase inhibitors. Total proteins or proteins of subcellular fractions were immunoprecipitated with the relevant antibody and separated by protein A/G-agarose. Protein samples were separated by standard SDS-PAGE and transferred onto nitrocellulose membrane. After blocking with 10% skimmed milk, the membranes were incubated overnight with primary antibodies followed by horseradish peroxidase-conjugated secondary antibodies.

VEGFR1 Visualization—PAECs stably expressing VEGFR1 (WT or V767A) tagged with GFP were grown to near confluence in 14-mm microwells in a 35-mm Petri dish (MatTek, Ashland, MA) and treated with growth factors for the indicated time periods. After treatment, the monolayers were fixed with 4% paraformaldehyde and permeabilized with 0.25% Triton X-100 for 5 min, and after blocking with 0.1% bovine serum albumin, cells were incubated for 1 h with anti-tubulin-TRITC antibody (Santa Cruz Biotechnology, Santa Cruz, CA) to illustrate the shape of the cells. Cells were then mounted using Vectashield (Vector Laboratories, Burlingame, CA) containing DAPI. Images were captured using an Olympus IX181-DSU confocal microscope (Olympus America, Center Valley, PA) operated by 3i's SlideBook™ software (Intelligent Imaging Innovations, Denver, CO).

siRNA Treatment—BRMECs were transfected with Stealth Select RNAi™ duplex oligoribonucleotides against VE-PTP (HSS108847, Invitrogen), SH-PTP1 (HSS140948, Invitrogen), SH-PTP2 (HSS108834, Invitrogen), PS1 (s224427, Invitrogen), NCT (s23706, Invitrogen), APH-1 (s27450, Invitrogen), and PEN-2 (s31661, Invitrogen) or with scrambled siRNA (12935-300, Invitrogen) for 48 h. The cells were changed to endothelial cell basal medium with growth supplement for 24 h (Invitrogen). Cells were than treated with growth factors as described above.

Association of VE-PTP, PS1, and NCT—BRMECs were treated with different growth factors in the presence or absence of γ-secretase inhibitors. 600 μl of cell lysates containing 500 μg of protein/ml for each treatment was divided into three equal portions. The three portions were immunoprecipitated with either rabbit anti-PTPRB (VE-PTP) (Abnova, Walnut, CA), goat anti-C terminus of PS1 (Santa Cruz Biotechnology), or mouse anti-NCT (Santa Cruz Biotechnology), respectively. Each of the three immunoprecipitates was then analyzed by Western blot using the same three antibodies.

Proximity Ligation Assay—BRMECs (2.0×10^4/well) were seeded into 14-mm microwells in a 35-mm Petri dish (MatTek). After 45 min in endothelial basal medium, cells were treated with different growth factors in the presence or absence of γ-secretase inhibitor for 10 min at 37 °C. Cultures were fixed in 4% paraformaldehyde, and after blocking for nonspecific binding, cells were incubated with the following primary antibodies: goat anti-human VEGFR1 (R&D Systems) and rabbit anti-PTPRB (VE-PTP) (Abnova). Secondary antibodies (anti-goat and anti-rabbit) conjugated with DNA probes (Olink Bioscience, Uppsala, Sweden) were added followed by ligation and circulation of DNA. After a rolling circle amplification, the reactions were detected by a complementary Texas Red-labeled DNA linker. The cells were mounted with Duolink II Mounting Medium containing DAPI (Olink Bioscience) and observed using an Olympus IX181-DSU confocal microscope (Olympus America) controlled by 3i's SlideBook™ software (Intelligent Imaging Innovations). We quantified the staining by morphometric evaluation according to the procedure of Pinto *et al.* (20). In brief, we selected 15 random regions per sample at ×400. An eyepiece with a systematic point sampling grid with 100 points and 50 lines was used to determine the fraction of points overlying the positive staining. We averaged this over 15 regions to obtain a final result as a percentage of the point fraction overlying staining.

VEGFR1 Phosphorylation Assay—BRMECs were cultured to confluence in 6-well plates. After 45 min in endothelial basal medium, cells were treated with different growth factors in the presence or absence of γ-secretase inhibitor (DAPT) for 10 min at 37 °C and then washed once in ice-cold phosphate-buffered

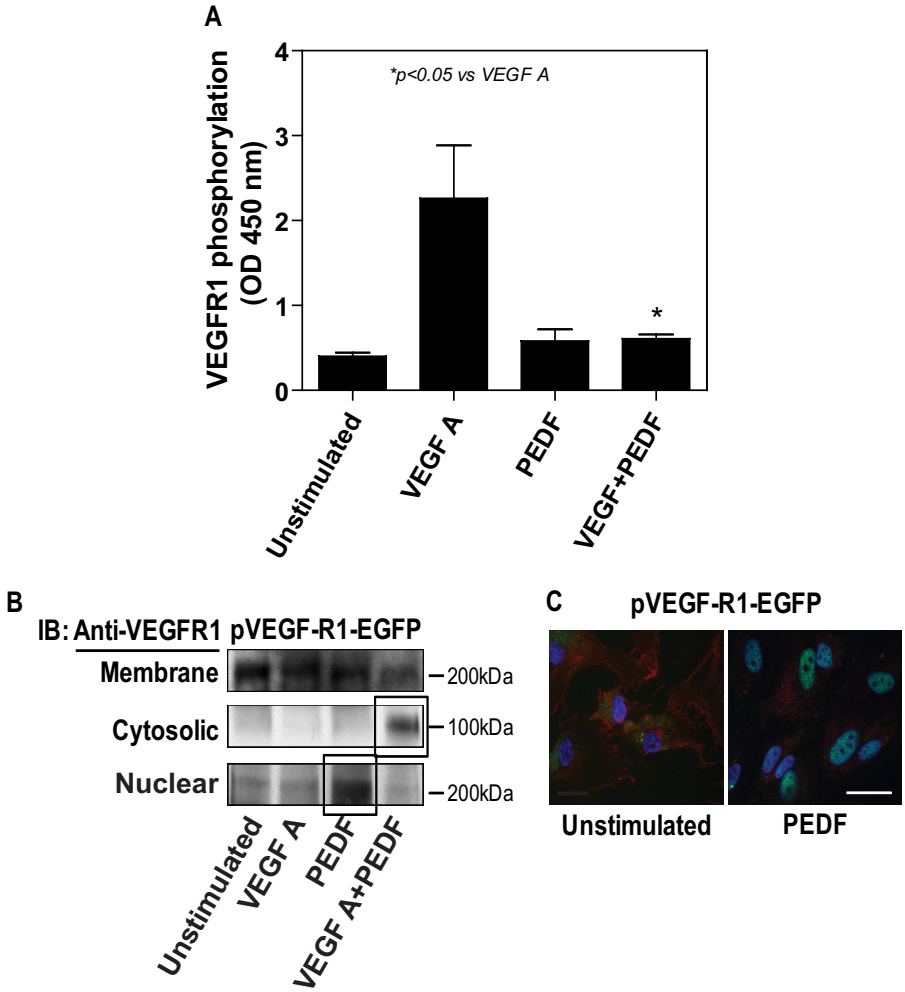

FIGURE 2. **VEGFR1-GFP-WT exhibits structural and functional characteristics of endogenous VEGFR1 receptors.** PAECs were stably transfected with VEGFR1-GFP-WT and treated with VEGF (100 ng/ml) and/or PEDF (100 ng/ml) for 24 h. *A*, ELISA showing that VEGF induced VEGFR1 phosphorylation and that this was blocked by PEDF. *Error bars* = S.E. *B*, representative Western blot analysis of subcellular fractions using antibody against the C terminus of VEGFR1 confirmed that PEDF + VEGF induced the appearance of a VEGFR1 fragment in the cytosol (*boxed*), whereas PEDF alone induced translocation of full-length VEGFR1 to the nucleus (*boxed*). *C*, cells were stained for tubulin (*red*) and nuclei (DAPI; *blue*). Cells were visualized by confocal fluorescence. In VEGFR1-GFP-WT cells, PEDF induced a nuclear translocation of VEGFR1. *, $p < 0.05$ *versus* VEGF. *Error bars* = S.E. *IB*, immunoblot.

saline. Phospho-VEGFR1 levels were determined with the human VEGFR1 DuoSet® IC enzyme-linked immunosorbent assay kit (R&D Systems). Enzyme-linked immunosorbent assay plates were coated with anti-human VEGFR1 and anti-human phosphorylated VEGFR1.

In Vitro Infection of AAV2-VE-PS1—A recombinant AAV serotype 2 quadruple tyrosine to phenylalanine capsid mutant (AAV2) containing VEcad promoter driving mouse PS1 cDNA was generated as described previously (21). A wild type AAV2 without the PS1 gene served as a control. BRMECs were grown in 24-well plates and infected with quadruple tyrosine mutant AAV2-VEcad-PS1 at 2×10^5 genomic particles/well and incubate at 37 °C for 3 days.

Statistical Analysis—All of the experiments were repeated at least three times. The results are expressed as the means ± S.E. VEGFR1 phosphorylation was analyzed using a Student's *t* test. The Mann-Whitney test was used to determine statistical significance of the laser densitometry data and the proximity ligation assay analysis.

RESULTS

VEGFR1-GFP-WT Exhibits Structural and Functional Characteristics of Endogenous VEGFR1 Receptors—To accurately identify the transmembrane cleavage site for VEGFR1, it was necessary to construct GFP-tagged VEGFR1 expression vectors and to express the fusion protein in a PAEC line devoid of VEGF receptors to avoid interference from endogenous VEGF receptors. We confirmed that this receptor was functional by showing that (*a*) VEGF induced phosphorylation of VEGFR1 (Fig. 2*A*), (*b*) an intracellular domain fragment of VEGFR1 was released when cells were treated with PEDF and VEGF (Fig. 2*B*), and (*c*) PEDF induced translocation of VEGFR1 to the nucleus (Fig. 2, *B* and *C*). This is in agreement with our previously published studies that showed activation of endogenous VEGFR1 in microvascular endothelial cells (7).

Site-directed Mutagenesis of Valine 767 to Alanine within VEGFR1 TMD Abolishes γ-Secretase-dependent Cleavage of VEGFR1—Because valine is known to be a critical amino acid for γ-secretase-dependent cleavage of the TMDs of many type

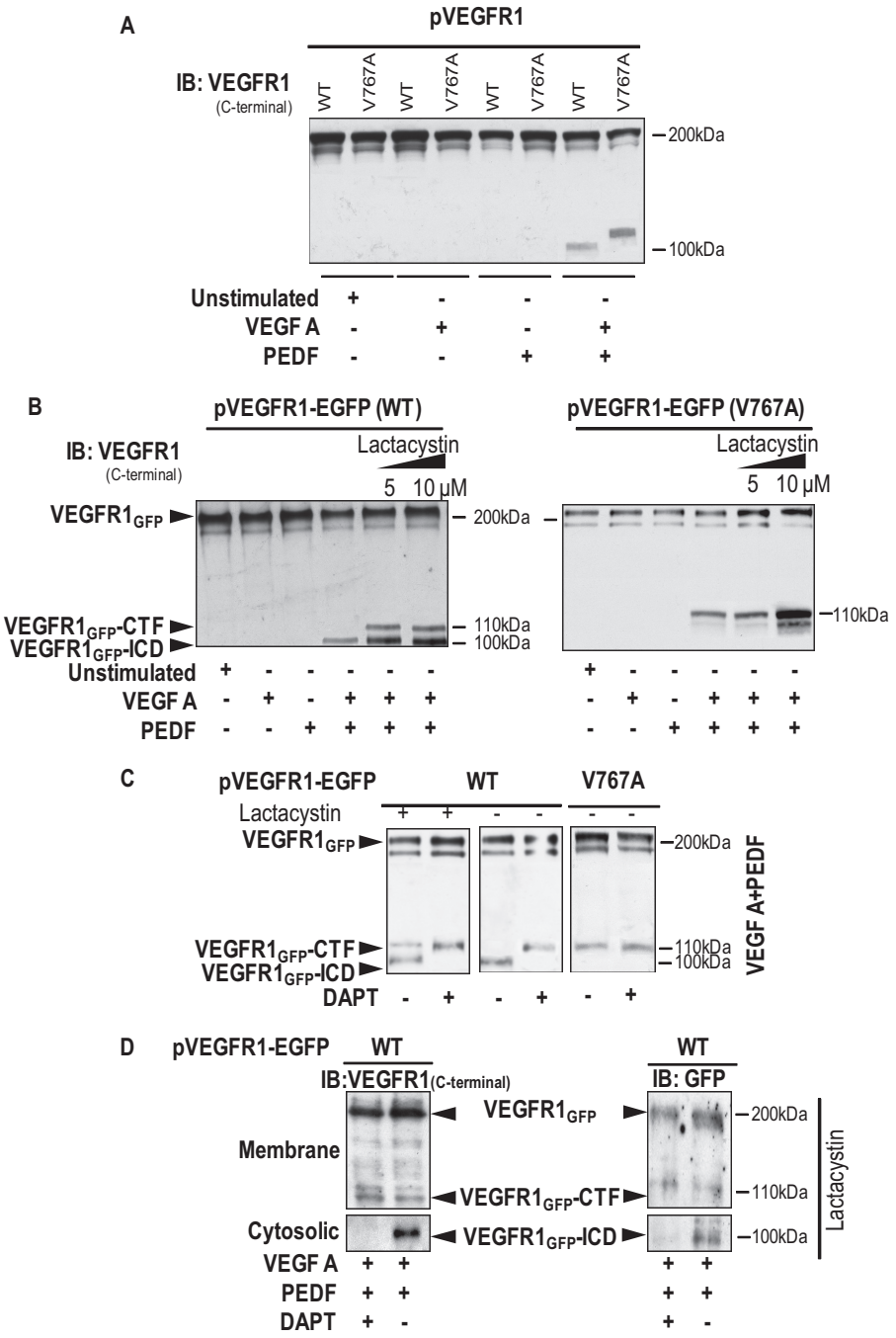

FIGURE 3. **Site-directed mutagenesis of valine 767 to alanine within VEGFR1 TMD abolishes γ-secretase-dependent cleavage of VEGFR1.** PAECs were stably transfected with VEGFR1-GFP-WT or mutant VEGF-GFP (V767A). *A*, PAECs were treated with VEGF (100 ng/ml) and/or PEDF (100 ng/ml) for 24 h. *B*, prior to VEGF/PEDF treatment, PAECs were incubated with proteasomal inhibitor (lactacystin) at the indicated doses for 5 h. *C*, PAECs stably expressing VEGFR1-GFP-WT were treated with 10 μM lactacystin or untreated for 10 h and then challenged with DAPT (10 μM) for 4 h. For *A–C*, the same amount of protein was resolved by 10% SDS-PAGE and analyzed by Western blot with an antibody against the C-terminal domain of VEGFR1. *D*, after treatments indicated in *C*, subcellular fractions (membrane and cytosolic) were prepared and subjected to Western blot analysis using antibody against the C terminus of VEGFR1 or GFP. *Arrows* indicate positions of full-length VEGFR1-GFP, VEGFR1-GFP-CTF, and VEGFR1-GFP-ICD. *IB*, immunoblot.

1 proteins, we tested whether valine 767 within the TMD of VEGFR1 is crucial for γ-secretase-dependent cleavage by stably transfecting PAECs with mutant VEGFR1-GFP (V767A). We treated PAECs expressing WT or mutant (V767A) VEGFR1-GFP with VEGF, PEDF, or a combination of both and undertook Western blot analysis using an anti-VEGFR1 antibody directed against the intracellular domain. Following the combination treatment of VEGF + PEDF, we detected the expected 100-kDa fragment (an 80-kDa cleaved peptide tagged with GFP) in the wild type cells, whereas by contrast, a ~110-kDa fragment was observed in V767A cells (Fig. 3*A*). In addition, a 200-kDa band representing full-length VEGFR1 was also observed in both PAEC cell lines. We postulated that the 110-kDa band represented a VEGFR1 fragment following ectodomain shedding but without subsequent γ-secretase cleavage that included a small TMD. We proposed that the absence of a

similar 110-kDa band in cells with WT VEGFR1 reflected the transient nature and rapid proteasomal degradation of the 110-kDa CTF. To confirm this, PAECs expressing wild type or mutant (V767A) VEGFR1 were treated with the proteasome inhibitor lactacystin. In wild type cells treated with VEGF + PEDF, lactacystin treatment allowed detection of the 100-kDa intracellular domain (ICD) plus an additional ~110-kDa CTF fragment that gained intensity at the highest concentration of lactacystin (Fig. 3*B*). In contrast, only ~110-kDa CTF was visualized in V767A cells even after treatment with lactacystin. Interestingly, a weak lower molecular weight band different from either CTF or ICD was observed at the highest lactacystin concentration that may reflect cleavage by α-secretase (*e.g.* ADAM10), which is known to be present in endothelial cells (22). No fragments were detected with antibody directed against the extracellular domain of VEGFR1 (data not shown), further confirming that the observed fragments are C-terminal fragments of VEGFR1. We next wished to determine whether treatment with the γ-secretase inhibitor DAPT had an effect on WT VEGFR1 similar to that observed for mutant VEGFR1. Indeed, DAPT caused an accumulation of VEGFR1-CTF and prevented cleavage to form a VEGFR1-ICD (Fig. 3*C*). Furthermore, subcellular fractionation and immunoblotting demonstrated the appearance of cytosolic VEGFR1-ICD in wild type cells receiving VEGF + PEDF treatment that was blocked by DAPT and absent in the mutant cells (Fig. 3*D*). On the basis of the sizes of these fragments, we estimated that the relevant cleavage of full-length VEGFR1 occurs near the extracellular juxtamembrane domain for generation of a ~110-kDa fragment and near the TMD for the 100-kDa fragment. These putative cleavage sites are consistent with the ectodomain shedding and γ-secretase cleavage observed for other type I membrane receptors (6).

VEGFR1 Serves as Substrate for VE-PTP, and This Is Facilitated by PS1—We have shown previously that PEDF also exerts γ-secretase-dependent regulation of VEGF-induced VEGFR1 phosphorylation (7). To investigate which subtype of PTP has a major role in PEDF-dependent VEGFR1 dephosphorylation, we transfected retinal endothelial cells with siRNA to knock down the expressions of SHP1, SHP2, or VE-PTP prior to treatment of cells with VEGF and/or PEDF. All siRNAs showed greater than 80% knockdown efficiency of their respective PTPs (Fig. 4*A*). Knockdown of SHP1 or SHP2 had no effect on the levels of VEGFR1 phosphorylation compared with the scrambled siRNA treatment in either untreated cells or cells receiving PEDF alone (Fig. 4*B*). However, the phosphorylation of VEGFR1 significantly increased (9–10-fold) across all treatment groups when the cells were transfected with VE-PTP siRNA compared with scrambled siRNA control. As expected, the cells treated with VEGF alone exhibited the same high levels of VEGFR1 phosphorylation under all conditions. PEDF was able to prevent VEGF-induced VEGFR1 phosphorylation, but this was reversed if VE-PTP was knocked down (Fig. 4*B*). This indicates that VE-PTP is necessary for PEDF to inhibit VEGF-induced phosphorylation of VEGFR1.

We used a proximity ligation assay, which allows the detection of molecular complexes *in situ*. As shown in Fig. 4*C* and quantified in Fig. 4*D*, VEGF prompted a modest formation of a VE-PTP·VEGFR1 complex, whereas addition of PEDF dramatically enhanced this complex formation. Unexpectedly, inhibition of γ-secretase using DAPT treatment did not reverse the effect of PEDF on the formation of the VE-PTP·VEGFR1 complex (Fig. 4*D*). Because our previous study indicated that the γ-secretase complex played a role in PEDF-regulated VEGFR1 dephosphorylation (7), we next determined whether individual components of the γ-secretase complex (*e.g.* PS1 or NCT) rather than the whole complex facilitated formation of the VE-PTP·VEGFR1 complex using co-immunoprecipitation and Western blotting (Fig. 4*C*). We observed that PEDF alone and PEDF + VEGF induced a strong association of full-length PS1 (Fl.PS1) but not the PS1 C-terminal fragment (PS1-CTF; which is normally associated with the γ-secretase complex) with VE-PTP (Fig. 4*E*). This association was not affected by DAPT inhibition of γ-secretase, suggesting that this involvement of PS1 is independent of γ-secretase activity. There was no association between nicastrin and VE-PTP (Fig. 4*E*). We did not observe an association between VE-PTP and the N terminus of PS1 (data not shown).

Full-length PS1 Regulates VEGFR1 Phosphorylation—Because PS1 has been reported recently to act as an adaptor molecule for the *N*-glycosylation of the vacuolar type ATPase V0a1 subunit (10), we postulated that the Fl.PS1 may also facilitate the formation of the VE-PTP·VEGFR1 complex. To investigate this, we transfected endothelial cells with siRNAs against the four components of the γ-secretase complex: PS1, NCT, APH-1, and PEN-2. After 96 h, cells were treated with VEGF and/or PEDF for 30 min followed by measurement of VEGFR1 phosphorylation using a phospho-VEGFR1 ELISA kit (Fig. 5*A*). PS1 knockdown completely abolished the inhibitory effect of PEDF on VEGF-induced VEGFR1 phosphorylation, whereas knockdown of NCT and APH-1 did not impact VEGFR1 phosphorylation. Overexpression of Fl.PS1 using an AAV2-VEcad-PS1 vector resulted in a greater than 5-fold increase in Fl.PS1 in endothelial cells (Fig. 5*B*) and complete blockade of VEGF-induced phosphorylation of VEGFR1 (Fig. 5*C*). Surprisingly, we found that PEN-2 knockdown and to a lesser extent APH-1 knockdown led to a marked decrease in VEGF-induced VEGFR1 phosphorylation even in the absence of PEDF (Fig. 5*A*). Because PEN-2 has been reported previously to regulate PS1 processing (6, 23), we next determined whether knockdown of PEN-2 or APH-1 would affect levels of Fl.PS1. As shown in Fig. 5*D*, knockdown of both PEN-2 and APH-1 caused a significant increase in Fl.PS1, and this was accompanied by decreased levels of PS1-CTF. Knockdown of PS1 resulted in an increase in expression of both mature and immature forms of NCT, whereas NCT knockdown had no significant effect on the expression of the other three components (Fig. 5*D*). We next assessed γ-secretase activity in the cell lysates of endothelial cells following knockdown of PS1, NCT, APH-1, or PEN-2, respectively, and found that all the siRNA treatments significantly reduced PEDF-induced γ-secretase activity by at least 50% and that PS1 knockdown exerted the greatest inhibition (Fig. 5*E*). Taken together with the data presented in Fig. 4, *C* and *D*, that show VEGFR1 association with VE-PTP, these results

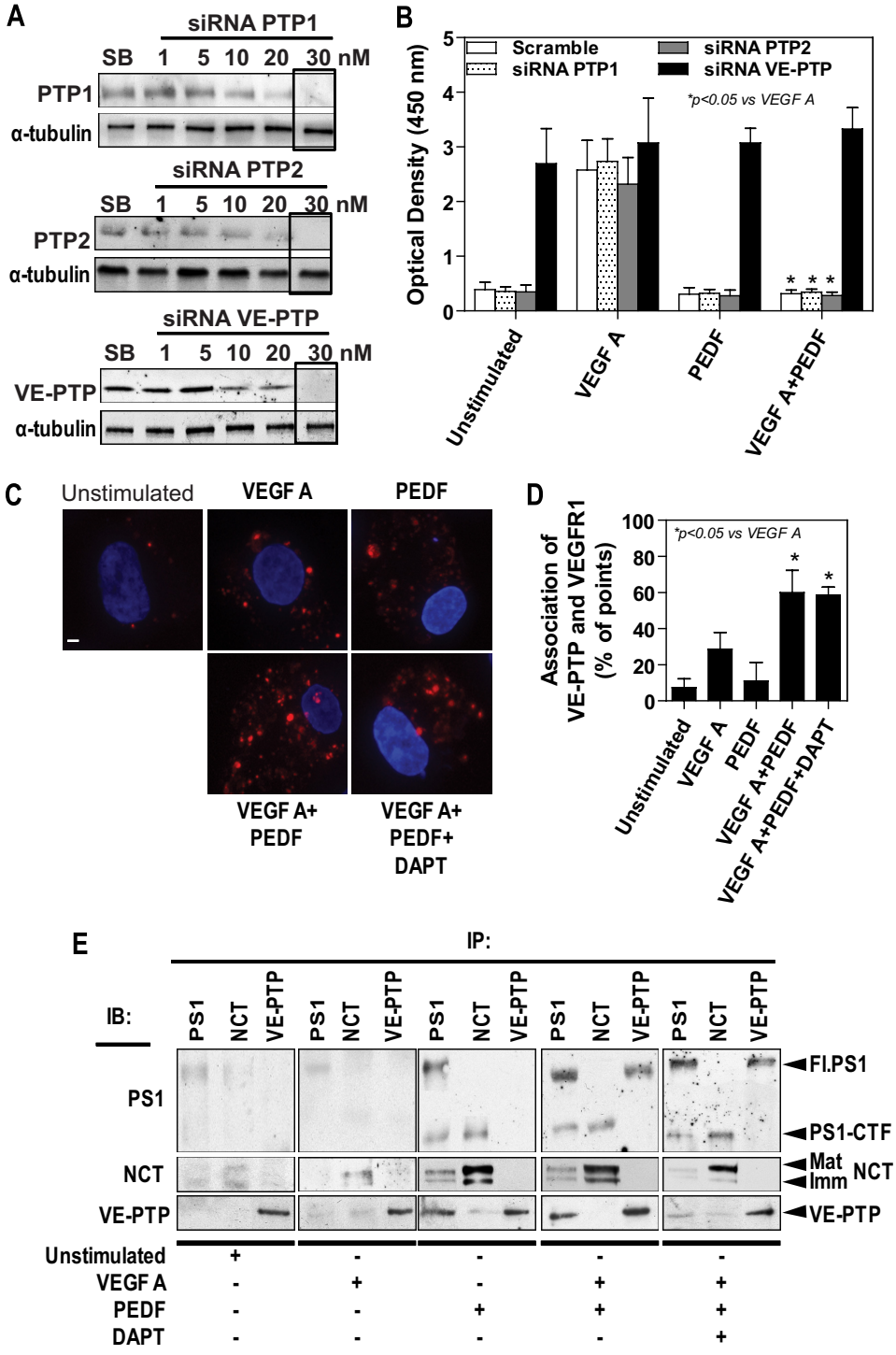

FIGURE 4. **VEGFR1 serves as substrate for VE-PTP and this is facilitated by PS1.** *A*, siRNA knockdown of PTP1, PTP2, or VE-PTP was optimized by Western blot analysis. *B*, retinal microvascular endothelial cells were transfected with scrambled siRNA or siRNA directed against PTP1, PTP2, or VE-PTP. 48 h post-transfection, cells were treated with VEGF (100 ng/ml) and/or PEDF (100 ng/ml) for 30 min, and VEGFR1 phosphorylation was assessed by ELISA. Only the knockdown of VE-PTP resulted in a significant increase in VEGFR1 phosphorylation. Results are shown as mean ± S.E. of three independent experiments. *C*, retinal microvascular endothelial cells were treated with VEGF (100 ng/ml) and/or PEDF (100 ng/ml) for 30 min with or without DAPT for 1 h. Detection of VE-PTP and VEGFR1 *in situ* was carried out by the proximity ligation assay. *Red* spots representing VE-PTP·VEGFR1 complexes show that PEDF increased the association of VE-PTP and VEGFR1. *Scale bar* = 10 μm. *D*, quantitation of proximity ligation assay staining. *E*, total lysates from cells treated as in *B* underwent co-immunoprecipitation/Western blotting using antibodies against VE-PTP, the C terminus of PS1, and NCT. *Arrows* indicate Fl.PS1, PS1-CTF, mature (*Mat*) and immature (*Imm*) forms of nicastrin, and VE-PTP. *, $p < 0.05$ *versus* VEGF. *Error bars* = S.E. *IP*, immunoprecipitation; *IB*, immunoblot; *SB*, scrambled siRNA.

suggest that Fl.PS1 may act as an adaptor to facilitate complex formation between VE-PTP and VEGFR1 and thus regulate VEGFR1 phosphorylation.

PEDF Enhances Binding of γ-Secretase Proteins and Fl.PS1 to VEGFR1 in Time-dependent Manner—Because we have already shown that constituents of the γ-secretase compo-

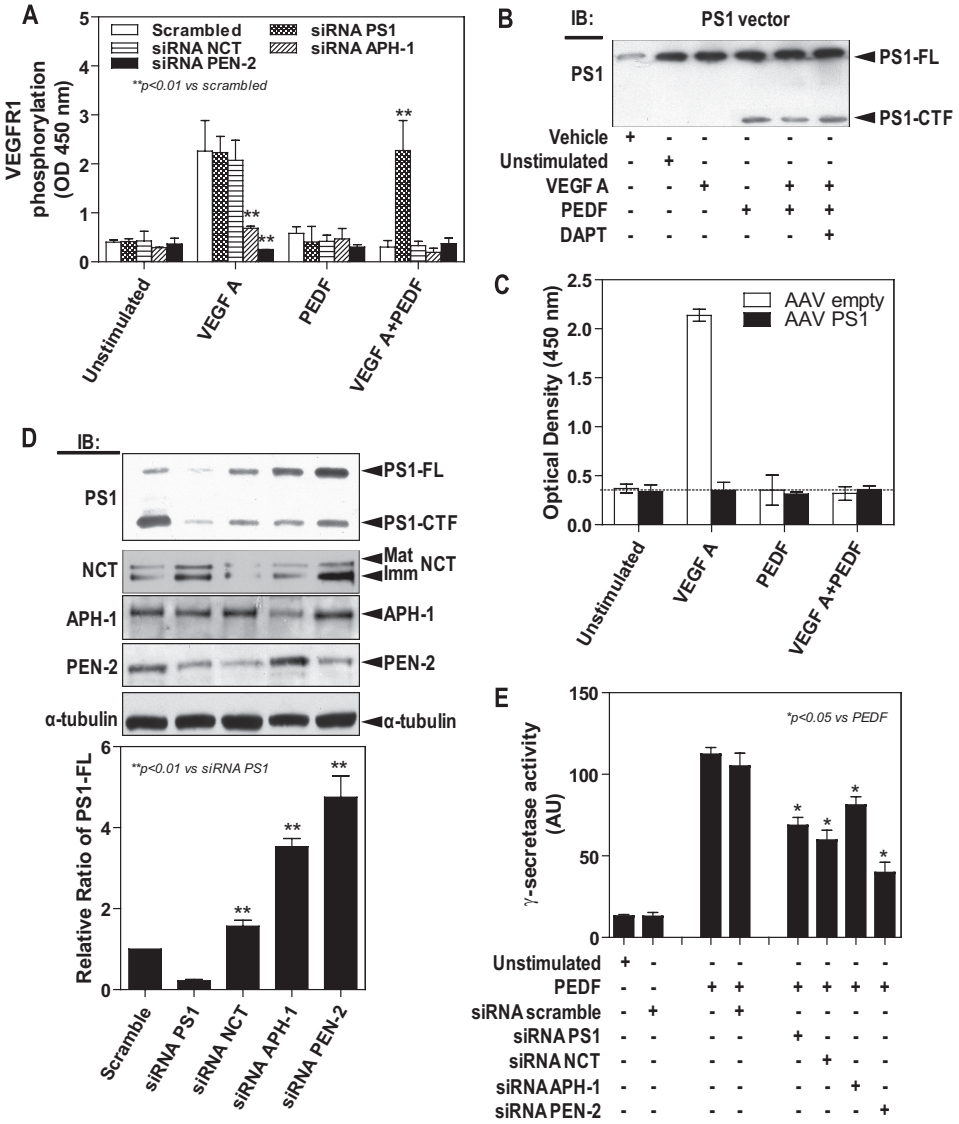

FIGURE 5. **Full-length PS1 regulates VEGFR1 phosphorylation by facilitating association of VEGFR1 and VE-PTP.** Retinal microvascular endothelial cells were transfected with scrambled siRNA or siRNA against PS1, NCT, APH-1, or PEN-2. 48 h post-transfection, cells were treated with VEGF A (100 ng/ml) and/or PEDF (100 ng/ml) for 30 min. *A*, VEGFR1 phosphorylation assay showed that knockdown of PS1 abolished the inhibitory effect of PEDF on VEGF-induced VEGFR1 phosphorylation, whereas knockdown of PEN-2 also resulted in a marked decrease in VEGF-induced VEGFR1 phosphorylation. **, $p < 0.01$ *versus* scrambled siRNA. *B*, retinal microvascular endothelial cells were infected with triple mutant AAV2 containing PS1 cDNA for 48 h, and the cells were treated with VEGF A (100 ng/ml) and/or PEDF (100 ng/ml). 24 h post-treatment, cell lysates were subjected to Western blot analysis using an antibody against the C terminus of PS1 and demonstrated high levels of Fl.PS1. *C*, the VEGFR1 phosphorylation assay of cells treated as in *B* confirmed that overexpression of PS1 greatly suppressed VEGFR1 phosphorylation regardless of growth factor treatment. *D*, Western blot analysis using antibodies against the C terminus of PS1, NCT, APH-1, or PEN-2, respectively, showed that siRNA knockdown of PS1 reduced levels of both Fl.PS1 and PS1-CTF with the greatest effect on Fl.PS1, whereas knockdown of PEN-2 significantly elevated Fl.PS1 levels. **, $p < 0.01$ *versus* siRNA PS1. *E*, measurement of γ-secretase activity showed that knockdown of each basic component of the γ-secretase complex significantly reduced γ-secretase activity. *, $p < 0.05$ *versus* PEDF. *Error bars* = S.E. *IB*, immunoblot; *AU*, absorbance units.

nents, in particular PS1, are involved in the RIP and regulation of phosphorylation of VEGFR1, we next determined the kinetics of γ-secretase component association with membrane-bound VEGFR1 in endothelial cells. To accomplish this, the membrane fractions of endothelial cells treated with VEGF and/or PEDF were immunoprecipitated with an antibody directed against the C terminus of VEGFR1 followed by Western blot using antibodies directed against each of the four components of γ-secretase (PS1, NCT, APH-1, and PEN-2) (Fig. 6). VEGF alone did not induce an increase in association of any of the components with VEGFR1. By contrast, PEDF stimulated a time-dependent association of the constituents of γ-secretase as well as Fl.PS1 with membrane-bound VEGFR1 (Fig. 6*B*). NCT and PEN-2 were associated with VEGFR1 within 15 min, and this was followed by APH-1 and the PS1-CTF, which associated with VEGFR1 within 30 min. Fl.PS1 associated with VEGFR1 as early as 15 min after PEDF treatment.

DISCUSSION

The present study revealed novel information on the role of the γ-secretase complex or its individual constituents in the regulation of VEGFR1 signaling. Specifically, we (*a*) identified the γ-secretase cleavage site within the TMD of VEGFR1 and (*b*) demonstrated that PS1 acts as an adaptor protein between

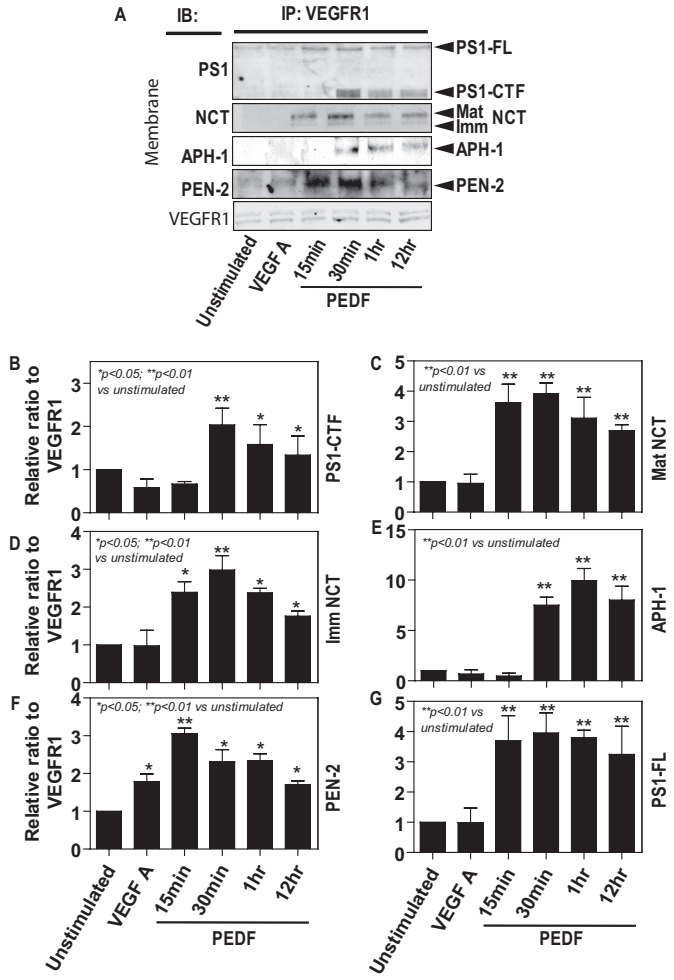

FIGURE 6. **PEDF enhances binding of γ-secretase proteins and Fl.PS1 to VEGFR1 in time-dependent manner.** Retinal microvascular endothelial cells were treated with VEGF (100 ng/ml) and/or PEDF (100 ng/ml) for the indicated periods of time. The total cell lysates were immunoprecipitated with antibody against the C terminus of VEGFR1 followed by Western blot analysis using antibodies against NCT, APH-1, PEN-2, and the C terminus of PS1, respectively. *A*, representative Western blot from three independent experiments. *B–G*, densitometric analysis of PS1-CTF, mature (*Mat*) and immature (*Imm*) NCT, APH-1, PEN-2, and Fl.PS1 relative to VEGFR1 from three independent experiments. *, $p < 0.05$; **, $p < 0.01$ *versus* unstimulated. *Error bars* = S.E. *IB*, immunoblot; *IP*, immunoprecipitation.

VE-PTP and VEGFR1 to facilitate dephosphorylation of VEGFR1.

The substrate sequences for γ-secretase cleavage of the TMD of a number of receptors including Notch and ErbB4 have been reported (13–15). Previous work has established that a valine residue(s) followed by charged residues within the TMD serve as cleavage sites for γ-secretase (24). Sequence alignments of the TMD of known γ-secretase substrates and VEGFR1 demonstrate the conservation of a valine residue within the TMD followed by charged residues immediately downstream of the TMD or juxtamembrane domain. Alignment of the TMD of VEGFR1 from a number of species revealed a complete homology in the TMD and conservation of valine (valine 767 in human VEGFR1) (Fig. 1). In the present study, we confirmed our prediction by demonstrating that a valine 767 to alanine 767 conversion in the TMD of VEGFR1 prevented γ-secretase cleavage of VEGFR1 and release of an intracellular domain. Although we cannot conclusively rule out an allosteric change to the mutant receptor, single valine to alanine substitutions have been undertaken in studies looking at other γ-secretase substrates, and there was no evidence of such a change affecting proteolysis.

As with other proteins undergoing RIP (25, 26), our data also highlight that newly generated VEGFR1 fragments are highly labile to proteasomal degradation. Proteasome inhibition led to the accumulation of a lower molecular weight VEGFR1-ICD and the appearance of the high molecular weight fragment in WT cells. Furthermore, Western blot analysis of subcellular fractions demonstrated that the high molecular weight fragment was located in the membrane fraction, whereas the lower molecular weight fragment was only found in the cytosolic fraction, indicating that the high molecular weight band represents the membrane-anchored VEGFR1-CTF (the resultant fragment from ectodomain cleavage), whereas the lower molecular fragment is the product of γ-secretase. The enzyme responsible for ectodomain cleavage of VEGFR1 has yet to be confirmed but may be mediated by ADAM10 (27).

We have reported previously that PEDF is able to mediate dephosphorylation of ligand-activated VEGFR1 (7). Here we show that VE-PTP is a major component of the VEGFR1 signaling pathway. PEDF caused rapid association of VE-PTP with VEGFR1, suggesting that this receptor type phosphatase represents a brake that PEDF can use to suppress VEGFR1 activity. siRNA experiments revealed that knockdown of VE-PTP significantly increased VEGFR1 phosphorylation. Very recently, it has been shown that VE-PTP dephosphorylates VEGFR2 in endothelial cells, and silencing VE-PTP expression leads to increased VEGFR2 phosphorylation with activation of downstream signaling pathways (28). Moreover, by association with vascular endothelial cadherin, VE-PTP can stabilize the low phosphorylation status of vascular endothelial cadherin and enhance vascular endothelial cadherin-dependent adhesion junctions in endothelial cells (19).

PS has been shown to regulate protein trafficking and protein-protein interactions independently of its protease activity and association with the γ-secretase complex even though the underlying mechanisms remain unclear (29–31). Some consensus exists that the mechanism involves the association between Fl.PS and transport proteins (32, 33). Indeed, a recent detailed study of PS interacting with β-catenin indicates that a GSK3β-induced structural change of the hydrophilic loop of Fl.PS1 leads to decreased phosphorylation and ubiquitination of β-catenin (34). We have now shown that Fl.PS1 acts as an adaptor to facilitate the association of VE-PTP with VEGFR1 as siRNA against PS1 abolished the inhibitory effect of PEDF on VEGF-stimulated VEGFR1 phosphorylation. It is also interesting to note that knockdown of PEN-2 resulted in a significant increase in the levels of Fl.PS1, which similarly led to a strong dephosphorylation of VEGFR1 in endothelial cells even without VEGF stimulation. These conclusions are supported by our finding that PS1 overexpression in endothelial cells that primarily elevates Fl.PS1 greatly suppressed VEGFR1 phosphorylation. It should be noted that γ-secretase activity does not necessarily correlate with siRNA knockdown of each its components. It has been reported previously that expression of

each component of the γ-secretase complex is coordinately regulated, and our data would support this. In the case of APH-1, our siRNA targeted APH-1αL because it has been suggested to be the dominant form of APH-1. However, recent studies report that multiple isoforms (αL, αS, and β) of APH-1 can replace each other in the γ-secretase complex (35, 36), and this may provide an explanation why our siRNA against APH-1 has less of an effect on γ-secretase activity. It has been shown that PS1 knockdown leads to a strong reduction of PEN-2 and that the PEN-2 level is also down-regulated upon siRNA knockdown of nicastrin (37). Furthermore, there is evidence that PEN-2 plays an important role in PS1 endoproteolysis (38). We speculate that knockdown of PEN-2 not only affects active γ-secretase formation but also reduces PS1 activation, leading to a further reduction in γ-secretase activity.

In conclusion, our findings reveal that PEDF mediates VEGFR1 signaling via (*a*) site-specific cleavage of the VEGFR1 TMD by γ-secretase and (*b*) PS acting as an adaptor protein to facilitate association of VE-PTP with VEGFR1 and thus promote dephosphorylation of VEGFR1. It is likely that these two signaling pathways can operate alone or in concert. The γ-secretase-dependent translocation of VEGFR1 to different intracellular locations plays a critical role in regulating cellular function (6–8). Furthermore, the phosphorylation status and kinase activity of proteins determine their ability to modulate both transcriptional and translational networks (39, 40). This greater understanding of the regulation of VEGFR1 signaling is of significant importance for cell biology and identifying novel anti-VEGF signaling therapeutic strategies.

REFERENCES

1. Kusari, J., Zhou, S. X., Padillo, E., Clarke, K. G., and Gil, D. W. (2010) *Invest. Ophthalmol. Vis. Sci.* **51,** 1044–1051
2. Kerbel, R. S. (2008) *N. Engl. J. Med.* **358,** 2039–2049
3. Olsson, A. K., Dimberg, A., Kreuger, J., and Claesson-Welsh, L. (2006) *Nat. Rev. Mol. Cell Biol.* **7,** 359–371
4. Rahimi, N. (2006) *Front. Biosci.* **11,** 818–829
5. Cai, J., Wu, L., Qi, X., Shaw, L., Li Calzi, S., Caballero, S., Jiang, W. G., Vinores, S. A., Antonetti, D., Ahmed, A., Grant, M. B., and Boulton, M. E. (2011) *PLoS One* **6,** e18076
6. Boulton, M. E., Cai, J., and Grant, M. B. (2008) *J. Cell. Mol. Med.* **12,** 781–795
7. Cai, J., Jiang, W. G., Grant, M. B., and Boulton, M. (2006) *J. Biol. Chem.* **281,** 3604–3613
8. Cai, J., Wu, L., Qi, X., Li Calzi, S., Caballero, S., Shaw, L., Ruan, Q., Grant, M. B., and Boulton, M. E. (2011) *PLoS One* **6,** e21164
9. Rahimi, N., Golde, T. E., and Meyer, R. D. (2009) *Cancer Res.* **69,** 2607–2614
10. Lee, J. H., Yu, W. H., Kumar, A., Lee, S., Mohan, P. S., Peterhoff, C. M., Wolfe, D. M., Martinez-Vicente, M., Massey, A. C., Sovak, G., Uchiyama, Y., Westaway, D., Cuervo, A. M., and Nixon, R. A. (2010) *Cell* **141,** 1146–1158
11. Repetto, E., Yoon, I. S., Zheng, H., and Kang, D. E. (2007) *J. Biol. Chem.* **282,** 31504–31516
12. Brown, M. S., Ye, J., Rawson, R. B., and Goldstein, J. L. (2000) *Cell* **100,** 391–398
13. Lieber, T., Kidd, S., and Young, M. W. (2002) *Genes Dev.* **16,** 209–221
14. Brou, C., Logeat, F., Gupta, N., Bessia, C., LeBail, O., Doedens, J. R., Cumano, A., Roux, P., Black, R. A., and Israël, A. (2000) *Mol. Cell* **5,** 207–216
15. Schroeter, E. H., Kisslinger, J. A., and Kopan, R. (1998) *Nature* **393,** 382–386
16. Adachi, M., Fischer, E. H., Ihle, J., Imai, K., Jirik, F., Neel, B., Pawson, T., Shen, S., Thomas, M., Ullrich, A., and Zhao, Z. (1996) *Cell* **85,** 15
17. Flint, A. J., Tiganis, T., Barford, D., and Tonks, N. K. (1997) *Proc. Natl. Acad. Sci. U.S.A.* **94,** 1680–1685
18. Zhao, B., Cai, J., and Boulton, M. (2004) *Microvasc. Res.* **68,** 239–246
19. Nottebaum, A. F., Cagna, G., Winderlich, M., Gamp, A. C., Linnepe, R., Polaschegg, C., Filippova, K., Lyck, R., Engelhardt, B., Kamenyeva, O., Bixel, M. G., Butz, S., and Vestweber, D. (2008) *J. Exp. Med.* **205,** 2929–2945
20. Pinto, C. A., Carvalho, P. E., Antonângelo, L., Garippo, A., Da Silva, A. G., Soares, F., Younes, R., Beyruti, R., Takagaki, T., Saldiva, P., Vollmer, R. T., and Capelozzi, V. L. (2003) *Clin. Cancer Res.* **9,** 3098–3104
21. Markusic, D. M., Herzog, R. W., Aslanidi, G. V., Hoffman, B. E., Li, B., Li, M., Jayandharan, G. R., Ling, C., Zolotukhin, I., Ma, W., Zolotukhin, S., Srivastava, A., and Zhong, L. (2010) *Mol. Ther.* **18,** 2048–2056
22. Schulz, B., Pruessmeyer, J., Maretzky, T., Ludwig, A., Blobel, C. P., Saftig, P., and Reiss, K. (2008) *Circ. Res.* **102,** 1192–1201
23. Wolfe, M. S. (2009) *Semin. Cell Dev. Biol.* **20,** 219–224
24. Taniguchi, Y., Kim, S. H., and Sisodia, S. S. (2003) *J. Biol. Chem.* **278,** 30425–30428
25. Foveau, B., Ancot, F., Leroy, C., Petrelli, A., Reiss, K., Vingtdeux, V., Giordano, S., Fafeur, V., and Tulasne, D. (2009) *Mol. Biol. Cell* **20,** 2495–2507
26. Marron, M. B., Singh, H., Tahir, T. A., Kavumkal, J., Kim, H. Z., Koh, G. Y., and Brindle, N. P. (2007) *J. Biol. Chem.* **282,** 30509–30517
27. Zhao, S., Gu, Y., Fan, R., Groome, L. J., Cooper, D., and Wang, Y. (2010) *Placenta* **31,** 512–518
28. Mellberg, S., Dimberg, A., Bahram, F., Hayashi, M., Rennel, E., Ameur, A., Westholm, J. O., Larsson, E., Lindahl, P., Cross, M. J., and Claesson-Welsh, L. (2009) *FASEB J.* **23,** 1490–1502
29. Scheper, W., Zwart, R., and Baas, F. (2004) *Brain Res. Mol. Brain Res.* **122,** 17–23
30. Kametani, F., Usami, M., Tanaka, K., Kume, H., and Mori, H. (2004) *Neurochem. Int.* **44,** 313–320
31. Dumanchin, C., Czech, C., Campion, D., Cuif, M. H., Poyot, T., Martin, C., Charbonnier, F., Goud, B., Pradier, L., and Frebourg, T. (1999) *Hum. Mol. Genet.* **8,** 1263–1269
32. Smith, S. K., Anderson, H. A., Yu, G., Robertson, A. G., Allen, S. J., Tyler, S. J., Naylor, R. L., Mason, G., Wilcock, G. W., Roche, P. A., Fraser, P. E., and Dawbarn, D. (2000) *Brain Res. Mol. Brain Res.* **78,** 100–107
33. Suga, K., Tomiyama, T., Mori, H., and Akagawa, K. (2004) *Biochem. J.* **381,** 619–628
34. Haapasalo, A., Kim, D. Y., Carey, B. W., Turunen, M. K., Pettingell, W. H., and Kovacs, D. M. (2007) *J. Biol. Chem.* **282,** 9063–9072
35. Chen, A. C., Guo, L. Y., Ostaszewski, B. L., Selkoe, D. J., and LaVoie, M. J. (2010) *J. Biol. Chem.* **285,** 11378–11391
36. Shiraishi, H., Marutani, T., Wang, H. Q., Maeda, Y., Kurono, Y., Takashima, A., Araki, W., Nishimura, M., Yanagisawa, K., and Komano, H. (2006) *Genes Cells* **11,** 83–93
37. Steiner, H., Winkler, E., Edbauer, D., Prokop, S., Basset, G., Yamasaki, A., Kostka, M., and Haass, C. (2002) *J. Biol. Chem.* **277,** 39062–39065
38. Takasugi, N., Tomita, T., Hayashi, I., Tsuruoka, M., Niimura, M., Takahashi, Y., Thinakaran, G., and Iwatsubo, T. (2003) *Nature* **422,** 438–441
39. Baek, S. H. (2011) *Mol. Cell* **42,** 274–284
40. Hunter, T. (2007) *Mol. Cell* **28,** 730–738